

Title:

Using Image Quality Metrics to quantifiably assess Super Resolution Reconstructions of Magnetic Image Resonance images.

Joanna Chappell⁴, Nada Mufti^{1,4}, Patrick O'Brien², George Attilakos², Magda Sokolska⁵, Priya Narayanan², Rosalind Aughwane¹, Giles Kendall^{1,2}, David Atkinson⁷, Sebastien Ourselin⁴, Anna L David^{1,2,8}, Andrew Melbourne^{4,5}

Affiliations:

1 Institute for Women's Health, University College London, UK. 2 University College London Hospital, UK. 3 Great Ormond Street Hospital for Children, UK 4 School of Biomedical Engineering and Imaging Sciences (BMEIS), King's College London, UK. 5 Dept. Medical Physics and Biomedical Engineering, University College London, UK. 6 Dept. Medical Physics and Biomedical Engineering, University College London Hospital, London, UK. 7 Centre for Medical Imaging, University College London, UK

Synopsis: (100 words)

Magnetic Resonance Images are increasingly being used for detection and diagnosis of Placental Complications¹. Here we apply this technology to reconstruction of placenta accreta spectrum. Super-Resolution Reconstruction (SRR) allows for a high-resolution 3D reconstruction from 2D MRI slices to allow for improved visibility of structures for future clinical use². The use of Image Quality metrics provides quantitative evaluation of the SRR images and allows comparisons to be drawn between the original 2D images and the SRR. These metrics are tested for statistical significance, providing an objective assessment of the SRR images.

Summary of main findings: (35 words)

There is a statistically significant difference in the image quality metrics between non-SRR MRI files and SRR files. Allowing for the potential of SRR images being used by clinicians in the diagnosis and treatment of placenta accrete spectrum disorders.

Abstract (850 words)**Introduction:**

Magnetic Resonance Imaging of the placenta is used within clinical practice for the diagnosis and management of placental complications.¹ MRI has the ability to provide quantitative measures relating to the tissue properties and function as well as the visualisation of the maternal and fetal blood vessels.² Interpreting MRI data can be complex and movement of both the mother and fetus can lead to image artefacts and distortion of the image features. In an effort to remove these errors and improve the visualisation of the image, Super-Resolution Reconstruction (SRR) can be used⁴. Super Resolution Reconstruction, is completed by reconstructing a high-resolution image from multiple, overlapping low-resolution images^{3,4}. There are qualitative methods of evaluating these reconstructions as to whether they improve the visualisation of the region of interest by ratings from clinical experts. The inclusion of quantitative methods of establishing statistical difference between the 2D MRI and the 3D reconstructions can improve the use of SRR and their future roles in detection and diagnosis clinically. This method is being increasingly used for visualisation of the fetal brain which is considered to be a rigid organ, use for placental diagnosis is still being explored due to the non-rigid nature of the organ. Use within late-gestation when there is less movement in utero allows for improved image quality.

The Peak Signal-to-Noise Ratio (PSNR) is an expression of the ratio between the maximum values of signal and the power of the distorting noise that affects the quality of the image, it is calculated as: ⁵

$$PSNR = 20\log_{10}\left(\frac{MAX_f}{\sqrt{MSE}}\right) \quad (1)$$

The Signal-to-Noise Ratio of an MR image is measured by taking the mean of a high-intensity region of interest and dividing by the standard deviation of the region of noise outside of the imaged object ⁵.

Structural Similarity Image metric (SSIM) measures the local structural similarity, by using a correlation between the quality and the perception of the human visual system. Instead of using traditional error summation methods, the SSIM models image distortion and contrast distortion ⁶.

Entropy is a statistical measure of the randomness that can be used to characterise the texture of the input image. It is a quantitative measure of the information transmitted in the image. It is defined as:

$$Entropy = - \sum_{i=1}^n p \cdot \log_2 p \quad (2)$$

Where p contains the normalised histogram counts ^{7,8,9}.

Methods:

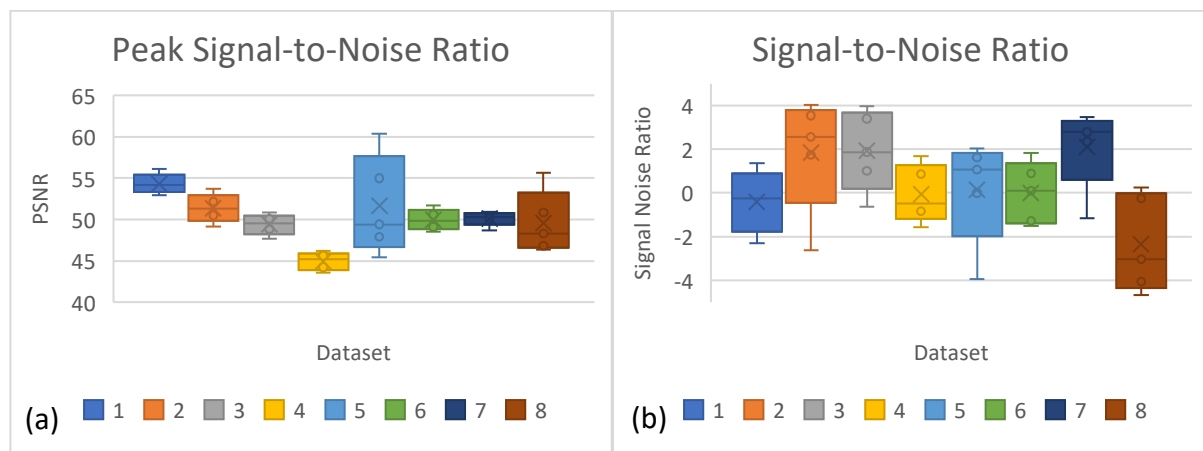
6 cases of suspected Placenta Accreta Spectrum Disorders by MRI, at late-stage gestation.

Imaging were performed on 1.5T Siemens Symphony, images were acquired in three orthogonal planes with TR/TE resolution and 50 slices.

A 3D super resolution reconstruction was completed for all of the datasets, using the method proposed by Ebner et al 2020⁴, followed by the SRR files being converted to 2D by exporting the files as DICOM files and cropping the original MRIs to the same dimensions as the new SRR. This conversion was completed so that the calculations of the Peak Signal to Noise Ratio (PSNR), the Signal to Noise Ratio (SNR), Structural Similarity Image Metric (SSIM) and Entropy could be completed. These Image Quality Metrics were chosen as they cover parameters which determine image quality; including contrast, resolution, noise, artifacts and distortion⁸. The PSNR and SNR quantify the ratio of noise to the signal power⁶. The SSIM quantifies the distortion and artifacts within the image⁶. The entropy measures how much information is transmitted in the image so can be a direct comparison of changes in the image quality.⁸

Results:

Figure 1 shows the Peak Signal-to-Noise Ratio and Signal-to-Noise Ratio of the datasets where the SRR are the denominators. As well as the Structural Similarity Image Metric for each of the datasets



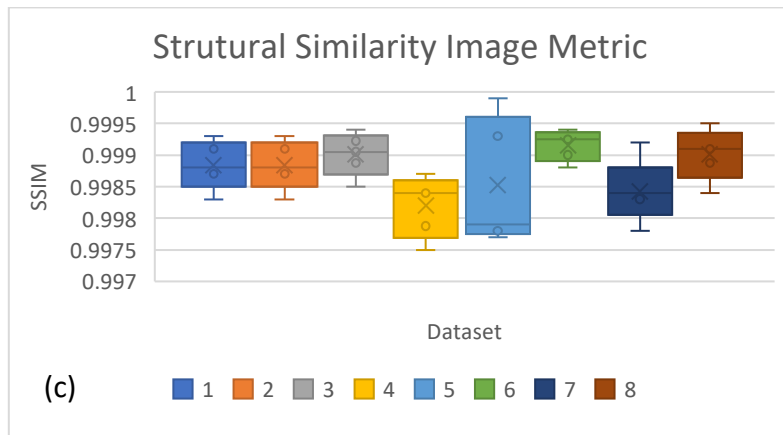
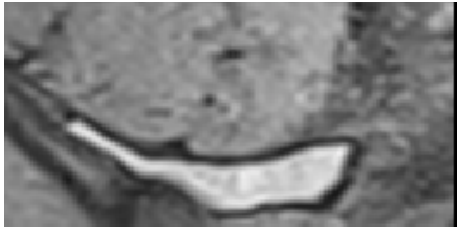
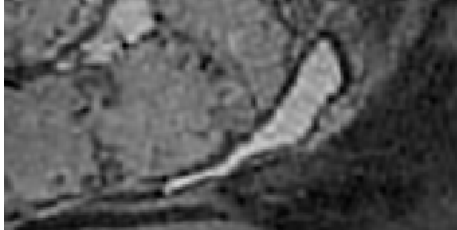
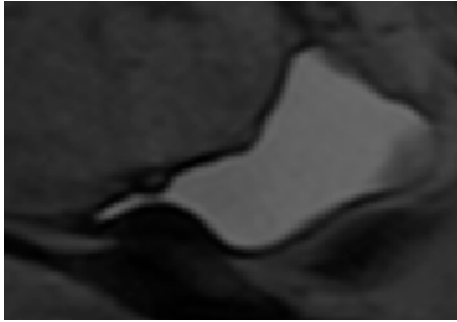

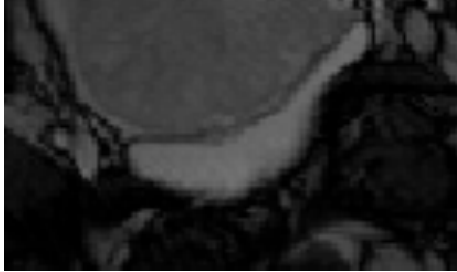







Figure 1: (a) The Peak Signal-to-Noise Ratio for each of the datasets (b) The Signal-to-Noise Ratio (c) The Structural Similarity Matrix for each of the datasets

Figure 2 shows the direct comparison of the 2D original MRI images and the SRR reconstruction images for visual observation. For each of the images the bladder is the Region of Interest

Datasets	Original	SRR
1		
2		

3		
4		
5		
6		
7		

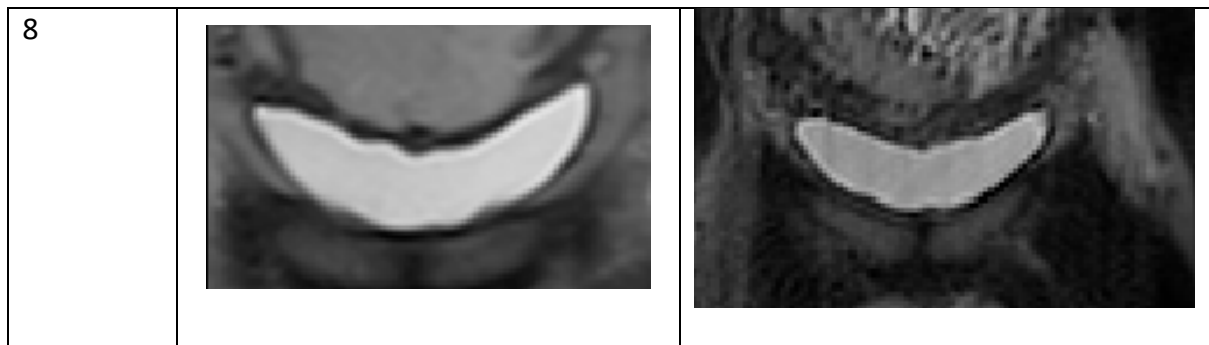


Figure 2: The Structural Similarity Image Metric for each of the datasets

Table 1 shows the entropy values for the cases along with the statistical significance calculations

Datasets	Entropy mean for the original	Entropy mean for the SRR	Statistical significance t-test value ($p < 0.05$)
1	0.2928	0.3878	6.013×10^{-5}
2	0.7427	0.9273	5.074×10^{-9}
3	0.9987	1.0816	1.822×10^{-44}
4	1.4525	1.5397	1.907×10^{-22}
5	0.1207	0.9673	2.622×10^{-8}
6	0.8017	1.0331	0.00807
7	1.0276	1.1988	2.809×10^{-6}
8	0.7107	0.9489	0.0197

Discussion:

In this study the 2D MRI images were compared to the 2D version of the 3D SRR images to establish if there is a quantifiable difference between the images.

The values found in our work correlate with previous findings from Gholipour et al ⁶ applied to the fetal brain that the PSNR and the quality of the image have a negative correlation when comparing the results within Figure 1 to the images within Figure 2.

However, there are limitations to the use of PSNR and SNR as both calculations make assumptions about the image intensity, which can lead to the discrimination of structural content in the images and degradations may not be picked up. The SSIM correlation within Figure 1 also illustrates this same point, however for all of the datasets the value can be rounded to 1, this may be due to the SSIM being correlated with the HVS colour model and all the images being grey scale. In order to address these limitations the PSNR, SNR and SSIM will be correlated to radiologist rating of the images, as well as the use of other Image Quality Metrics which will also allow for direct evaluation between the 2D original image and 3D reconstruction without the requirement to convert the image.

It can be seen from Table 1 that the entropy values for each of the cases shows statistical significance that the images are statistically different for all of the datasets, when a 2 tailed t-test was completed.

Conclusion:

This study uses a variety of image quality metrics to establish if there is a difference in super-resolution reconstruction images which have been exported to be 2D. The quantitative evaluation of the MR images shows that Super Resolution Reconstruction is enhancing the quality of the images, which may lead to the utilisation within the diagnosis and treatment of placenta accrete spectrum disorder.

References:

1. Aughware, R. et al. *Placental MRI and its application to fetal intervention*. Prenatal Diagnosis, 2020. **40**(1): p. 38-48
2. Melbourne, A. Aughwane, R. et al. *Separating fetal and maternal placental circulations using multiparametric MRI*. Magnetic Resonance in Medicine, 2019. **81**(1): p.350-361
3. Torrents-Barrena, J et al. *Fully Automatic 3D Reconstruction of the Placenta and its Peripheral Vasculature in Intrauterine Fetal MRI*. Med Image Anal, 2019. **54**(1): p. 263-279
4. Ebner, M et al. *An automated framework for localization, segmentation and super-resolution reconstruction of fetal brain MRI*. Neuroimage, 2020. **206**(1)
5. Plenge, E. Poot, D. Niessen, W. Meijering, E. *LNCS 8151 – Super-Resolution Reconstruction Using Cross-Scale Self-similarity in Multi-slice MRI*. MICCAI, 2013: p. 123-130
6. Gholipour, A. et al. *Super-resolution reconstruction in frequency, image and wavelet domains to reduce through-plane partial voluming in MRI*. Medical Physics, 2015. **42**(12): p. 6919-6932.
7. Obuchowicz, R. et al. *Magnetic Resonance Image Quality Assessment by Using Non-Maximum Suppression and Entropy Analysis*. Entropy, 2020. **22**(2): p. 220
8. Tsai, D. Lee, Y and Matsuyama, E. *Information Entropy Measure for Evaluation of Image Quality*. Journal of Digital Imaging, 2008. **21** (2): p. 338-347.
9. Ji, Q. Glass, J. Reddick, W. *A novel, fast entropy-minimization algorithm for bias field correction in MR images*. Magn Reson Imaging, 2007. **25**(2): p. 259-264